《原子核物理评论》
www.npr.ac.cn Nuclear Physics Review
Started in 1984

基于壳模型对力加四极力研究*sd*和*pf*壳偶偶原子核

贺冶秋　傅冠健

Shell Model Study of Even-even *sd* and *pf* Shell Nuclei With the Pairing Plus Quadrupole-quadrupole Interaction

HE Yeqiu, FU Guanjian

在线阅读 View online: https://doi.org/10.11804/NuclPhysRev.37.2019CNPC10

引用格式:
贺冶秋, 傅冠健. 基于壳模型对力加四极力研究*sd*和*pf*壳偶偶原子核[J]. 原子核物理评论, 2020, 37(3):509-515. doi: 10.11804/NuclPhysRev.37.2019CNPC10
HE Yeqiu, FU Guanjian. Shell Model Study of Even-even *sd* and *pf* Shell Nuclei With the Pairing Plus Quadrupole-quadrupole Interaction[J]. Nuclear Physics Review, 2020, 37(3):509-515. doi: 10.11804/NuclPhysRev.37.2019CNPC10

Article ID: 1007-4627(2020)03–0509–07

Shell Model Study of Even-even *sd* and *pf* Shell Nuclei With the Pairing Plus Quadrupole-quadrupole Interaction

HE Yeqiu, FU Guanjian†

(*School of Physics Science and Engineering, Tongji University, Shanghai 200092, China*)

Abstract: In this paper we study low-lying states of even-even nuclei in the *sd* and *pf* shells in the framework of the shell model with the phenomenological pairing plus quadrupole-quadrupole (P+Q) interaction. By adopting the single-particle energy and the monopole interaction from the USDB and GXPF1 interactions, the low-lying spectra of spherical nuclei and deformed nuclei are successfully reproduced by a unified set of parameters. We obtain a reasonably good result for binding energies by removing the monopole component from the pairing interactions. The isoscalar pairing interaction does not play an important role in the states. The monopole interaction provides contributions to the empirical proton-neutron interaction, the symmetry energy, and the Wigner energy.

Key words: shell model; P+Q interaction; unified parameter; monopole component

CLC number: O572.33 **Document code:** A **DOI:** 10.11804/NuclPhysRev.37.2019CNPC10

1 Introduction

The nuclear shell model is one of the most successful microscopic nuclear structure models[1]. In the shell model, the quantum many-body problem becomes diagonalizing a Hamiltonian matrix in a space spanned by multi-nucleon configuration basis states, with the assumption that valence protons and neutrons occupy several single-particle states. A shell-model effective Hamiltonian includes single-particle energies and two-body interactions. Many efforts have been devoted to description of low-lying states of atomic nuclei using the shell model with realistic nucleon-nucleon interaction, based on various renormalization and core polarization correction approaches[2–4]. Compared with experimental data, shell-model calculations with these realistic interactions deteriorate as the number of valence nucleons increases. Thus empirical corrections or fitting of an effective interaction are necessary[5–9]. Here we mention two typical types of interactions: the effective two-body-matrix-element (ETBME) Hamiltonian and the phenomenological P+Q interaction (*i.e.* the pairing plus quadrupole-quadrupole interaction).

An ETBME Hamiltonian is specified by a number of parameters, *i.e.*, single-particle energies and two-body matrix elements (TBMEs), in a given single-particle space. A few linear combinations of these parameters are derived from the least square fit, while the remaining linear combinations are fixed by a realistic interaction. This approach is successfully applied to obtain a few famous ETBME Hamiltonians, such as the USD, USDA, and USDB interactions in the *sd* shell[5–6], the GXPF1 interaction in the *pf* shell[7], and the JUN45 interaction in the $1p_{3/2}0f_{5/2}1p_{1/2}0g_{9/2}$ shell[8]. The advantage of the ETBME Hamiltonians is that interpolations and predictions for low-lying states are accurate. The drawbacks are that in higher shell regions there are too many TBMEs to evaluate and the configuration space is too gigantic to handle with the present computational ability, and it is not easy to figure out the physical meaning from the parameters.

The advantage of the P+Q interaction is that it has much less independent parameters and provides us with transparent pictures in physics. Due to its simplicity, the P+Q interaction has been extensively used to study low-lying states in nuclear structure models[10–22]. It has been demonstrated to be a reasonable approximation of the effective interaction for

Received date: 14 Dec. 2019; **Revised date:** 19 Mar. 2020

Foundation item: National Key R&D Program of China(2018YFA0404403); National Natural Science Foundation of China(12075169, 11605122)

Biography: HE Yeqiu(1987–), male, Shanghai, Master of Science, working on nuclear physics

† **Corresponding author:** FU Guanjian, E-mail: gjfu@tongji.edu.cn.

low-lying collective states, but unfortunately the fitting parameters vary widely for different nuclei in the same single-particle space.

In this work, we study low-lying states of nuclei in the *sd* and *pf* shells using the shell model with the phenomenological P+Q interaction. We shall show that by considering the "correct" monopole Hamiltonian, low-lying states of even-even nuclei can be well described by a unified set of parameters of the P+Q interaction. We shall also show that the pairing interaction is not independent of the monopole interaction; by removing the monopole component from the pairing interaction, the deviation of calculated binding energies from experimental data shall be reduced. This paper is organized as follows. In Sec. 2 we introduce the P+Q interaction and the parameters used in our shell-model calculation. In Sec. 3 we study low-lying states and binding energies, and extract the symmetry energy and Wigner energy coefficients. In Sec. 4 we summarize our results.

2 The P+Q interaction

The P+Q interaction is given as follows.

$$H_{\rm P+Q} = H_0 + V_{\rm m} + V_{\rm Q} + V_{P0} + V_{P2}. \tag{1}$$

The first term

$$H_0 = \sum_j \varepsilon_j \sum_{m\tau} a^\dagger_{jm\tau} a_{jm\tau}, \tag{2}$$

is the single-particle energy, and the second term is the monopole interaction[23], which is written as

$$V_{\rm m} = \sum_{JT} \sum_{j_1 \leqslant j_2} \frac{V_T(j_1 j_2) \sum_{m\tau} A^{JT}_{m\tau}(j_1 j_2)^\dagger A^{JT}_{m\tau}(j_1 j_2)}{\sqrt{(1+\delta_{j_1 j_2})(1+\delta_{j_3 j_4})}}, \tag{3}$$

$$V_T(j_1 j_2) = \frac{\sum_J V_{JT}(j_1 j_2 j_1 j_2)(2J+1)[1-(-)^{J+T}\delta_{j_1 j_2}]}{(2j_1+1)[(2j_2+1)+(-)^T \delta_{j_1 j_2}]}, \tag{4}$$

where $V_{JT}(j_1 j_2 j_1 j_2)$ is the TBME. The single-particle energy and monopole interaction represent the spherical single-particle mean field in the framework of the shell model, and play a dominant role in describing binding energies of atomic nuclei[1, 23–24]. The third term is the quadrupole-quadrupole interaction

$$V_Q = \kappa (Q_\pi + Q_\nu) \cdot (Q_\pi + Q_\nu), \tag{5}$$

where Q is the quadrupole operator, and κ is a parameter. The quadrupole-quadrupole interaction generates rotational motions and quadrupole deformations in a nucleus. The fourth and fifth terms are the isovector monopole and quadrupole pairing interactions, respectively, *i.e.*,

$$V_{P0} = G_0 \sum_\tau A^{(01)^\dagger}_{0\tau} A^{(01)}_{0\tau}, \tag{6}$$

$$V_{P2} = G_2 \sum_{m\tau} A^{(21)^\dagger}_{m\tau} A^{(21)}_{m\tau}, \tag{7}$$

where $A^{(JT)^\dagger}_{m\tau}$ is a creation operator of a collective nucleon pair with spin J and isospin T, and G_J is a parameter. In this work we also investigate the isoscalar $J=1$ and $J=2j_{\rm max}$ pairing interactions, *i.e.*,

$$V_{P1} = G_1 \sum_m A^{(10)^\dagger}_{m0} A^{(10)}_{m0}, \tag{8}$$

$$V_{P\rm max} = G_{\rm max} \sum_m A^{(2j_{\rm max}0)^\dagger}_{m0} A^{(2j_{\rm max}0)}_{m0}. \tag{9}$$

The pairing interactions defined in Eqs. (6)~(9) are not independent of the monopole interaction. Thus we remove the monopole component from V_{P0}, V_{P2}, V_{P1}, and $V_{P\rm max}$, and the modified pairing interactions are denoted by V'_{P0}, V'_{P2}, V'_{P1}, and $V'_{P\rm max}$, respectively. Meanwhile, the monopole-removal P+Q interaction should be written as

$$H'_{\rm P+Q} = H_0 + V_{\rm m} + V_{\rm Q} + V'_{P0} + V'_{P2}. \tag{10}$$

3 Calculations and results

We study yrast states of even-even nuclei in the *sd* shell and the *pf* shell, using the shell model with the P+Q interaction. The NuShellX shell-model code is used[25]. In order to obtain reasonable spherical mean field, the single-particle energy, H_0, and the monopole interaction, $V_{\rm m}$, are directly taken from ETBME Hamiltonians; here we adopt the USDB interaction[6] for the *sd* shell and the GXPF1 interaction[7] for the *pf* shell.

The parameters G_J and κ for the *sd* shell are optimized by fitting the excitation energy data of yrast even-J states for even-even nuclei $^{18\text{-}24}$O, $^{20\text{-}28}$Ne, $^{24\text{-}30}$Mg, $^{28\text{-}34}$Si, $^{32\text{-}36}$S, ^{36,38}Ar, and those for the *pf* shell are optimized by fitting the data for $^{42\text{-}48}$Ca, $^{44\text{-}50}$Ti, $^{48\text{-}52}$Cr. The detailed procedure is as follows. We define the weighted root-mean-square deviation of the excited energies between the calculations and experiments by

$$\sigma^2 \equiv \frac{\sum_i w_i (E^{\rm cal}_{x,i} - E^{\rm expt}_{x,i})^2}{\sum_i w_i}. \tag{11}$$

Here we take $w_i = 1.5, 1.3, 1.2, 1.1, 0.9, 0.5$ for the 2^+, 4^+, 6^+, 8^+, 10^+, 12^+ states, respectively. Our goal is to find the set of G_J and κ for which σ^2

reaches a minimum value. Here we make use of the conjugate gradient method[26–27], an iterative algorithm for unconstrained optimization problems, which we describe it as follows.

(1) We define the parameter vector $\vec{p}=\{p_1, p_2, \ldots, p_n\}$ where n is the number of parameters (*e.g.*, $\{G_0, G_2, \kappa\}$ for $H_{\rm P+Q}$), and σ^2 is the function of $\boldsymbol{p}$. We denote the initial guess for $\boldsymbol{p}$ by $\boldsymbol{p}_0$.

(2) We compute the negative gradient of σ^2 at $\boldsymbol{p}_0$, denoted by $-\boldsymbol{g}_1$, and use it as our initial search direction $\boldsymbol{d}_1$. The selection of the search direction will change in further iterations.

(3) Going from $\boldsymbol{p}_0$ in the direction of $\boldsymbol{d}_1$, we search for the solution $\boldsymbol{p}_1=\boldsymbol{p}_0+x_1\boldsymbol{d}_1$ for which σ^2 reaches the local minimum. The solution $\boldsymbol{p}_1$ is assumed to be the initial vector of the next iteration.

We repeat steps 2 and 3 until convergence, except that the search direction in the ith iteration $\boldsymbol{d}_i=-\boldsymbol{g}_i+\vec{d}_{i-1}|\boldsymbol{g}_i|^2/|\boldsymbol{g}_{i-1}|^2$.

Table 1 presents the parameters G_J and κ of $H_{\rm P+Q}$, $H'_{\rm P+Q}$ and $H'_{\rm P+Q}+V'_{P1}$ for the *sd* and *pf* shells. The values of G_0, G_2 and κ are a little different from those given in Refs. [28–29] ($G_0, G_2, \kappa \approx -0.40, -0.10, -0.66$ MeV for the *sd* shell, and $-0.48, -0.18, -0.15$ MeV for the *pf* shell). We calculate a few TBMEs with $J=0$ and $T=1$ of our P+Q interactions. For example, we obtain $V_{01}(d_{3/2}d_{3/2}d_{3/2}d_{3/2})=-1.57$ MeV, $V_{01}(d_{5/2}d_{5/2}d_{5/2}d_{5/2})=-2.21$ MeV, $V_{01}(f_{7/2}f_{7/2}f_{7/2}f_{7/2})=-2.26$ MeV for $H'_{\rm P+Q}$; these values are reasonably close to those given in the USDB and GXPF1 interactions ($-1.90, -2.56, -2.24$ MeV).

Table 1　The parameters (in the unit of MeV) of the pairing interactions, G_J, and the quadrupole-quadrupole interaction, κ, determined by fitting the excitation energy data in the *sd* and *pf* shells. All the parameters given in the table should be multiplied by $(\frac{A}{18})^{-0.3}$ in the *sd* shell and by $(\frac{A}{42})^{-\frac{1}{3}}$ in the *pf* shell.

Interaction	G_0	G_2	G_1	κ
		sd shell		
$H_{\rm P+Q}$	–0.182	–0.056		–0.513
$H'_{\rm P+Q}$	–0.194	–0.118		–0.512
$H'_{\rm P+Q}+V'_{P1}$	–0.197	–0.114	–0.049	–0.511
		pf shell		
$H_{\rm P+Q}$	–0.477	–0.108		–0.113
$H'_{\rm P+Q}$	–0.461	–0.116		–0.117
$H'_{\rm P+Q}+V'_{P1}$	–0.451	–0.109	–0.322	–0.107

3.1　The low-lying spectrum

Let us begin with the discussion of the low-lying spectrum. The yrast states of the even-even nuclei are well described by our shell-model calculation with the P+Q interaction. We exemplify this with the cases of ^{20}O, ^{20}Ne, ^{22}Ne, ^{24}Mg, and ^{28}Si in the *sd* shell (see in Fig. 1). ^{20}O is a typical semimagic nucleus with a spherical shape, and ^{20}Ne, ^{22}Ne, ^{24}Mg, ^{28}Si are deformed nuclei with a ground rotational band. The excitation energies obtained by $H_{\rm P+Q}$, $H'_{\rm P+Q}$, and $H'_{\rm P+Q}+V'_{P1}$ are all in good agreement with the data or the USDB results. The root-mean-square deviation of the excitation energies between the $H'_{\rm P+Q}$ results and the experimental data is 0.51 MeV, and that for the USDB interaction is 0.46 MeV. The monopole component in the pairing interactions and the isoscalar $J=1$ pairing interaction are not crucial in reproducing the low-lying spectra. The strength of the isoscalar $J=1$ pairing interaction, G_1, is small.

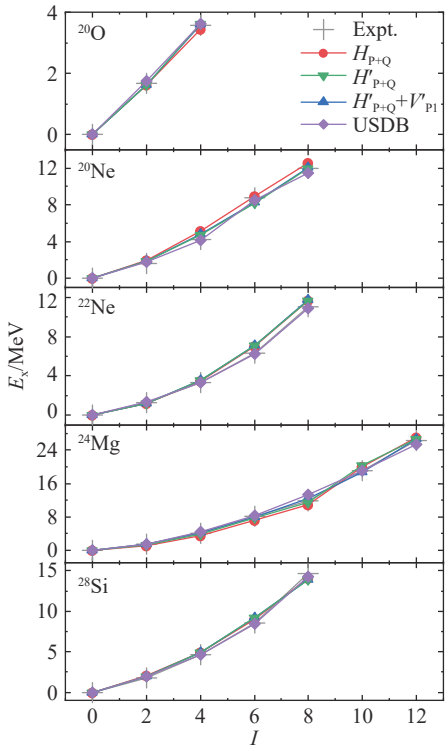

Fig. 1　(color online) Excitation energies of the yrast states of ^{20}O, ^{20}Ne, ^{22}Ne, ^{24}Mg, and ^{28}Si obtained from experimental data and by shell-model calculations with different interactions in the *sd* shell.

Similar results are found for the *pf*-shell nuclei. Fig. 2 compares for the yrast states of ^{44}Ca, ^{44}Ti, ^{46}Ti, ^{48}Cr, and ^{52}Fe the experimental data and the shell-model results. The excitation energies obtained by $H_{\rm P+Q}+V_{P1}$, $H'_{\rm P+Q}$, and $H'_{\rm P+Q}+V'_{P1}$ are all in good agreement with the GXPF1 results. The root-mean-square deviation of the excitation energies between the $H'_{\rm P+Q}$ results and the experimental data is 0.37

MeV and that for the GXPF1 interaction is 0.57 MeV (we exclude the 10^+ and 12^+ states of ^{44}Ti, due to the large discrepancy, in the calculation of the root-mean-square deviation). It is worth mentioning that the data of ^{52}Fe are not used in the parameter fitting, and our prediction for ^{52}Fe is good. The above result indicates the monopole component in the pairing interactions and the isoscalar $J=1$ pairing interaction do not play an important role here. In Table 1 we find the optimized parameter G_1 of $H'_{\rm P+Q}+V'_{P1}$ in the pf shell is not small, this can be explained as follows: the excitation energies are not sensitive to the G_1-parameter variation, and the value can be regarded as a result of overfitting.

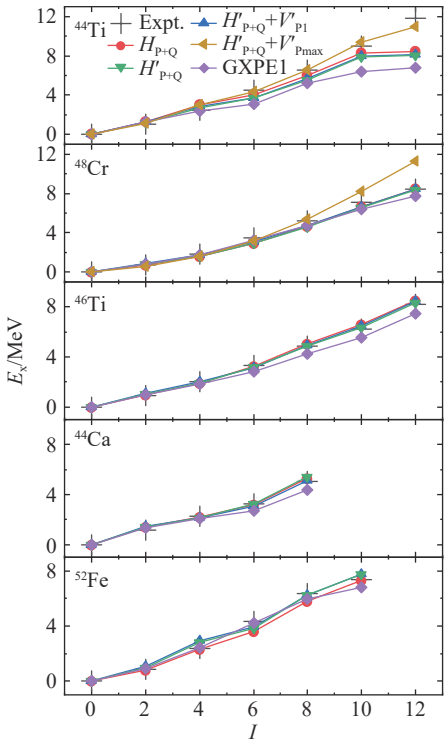

Fig. 2 (color online) Same as Fig. 1 except for ^{44}Ca, ^{44}Ti, ^{46}Ti, ^{48}Cr, and ^{52}Fe in the pf shell.

We also investigate $V'_{P\rm max}$, namely the isoscalar spin-aligned $J=7$ pairing interaction, in the pf shell calculation. The result of Ref. [30] shows that the quadrupole-quadrupole interaction is correlated with the $V_{P\rm max}$ interaction, and the wave functions generated by the pure quadrupole-quadrupole interaction and by the strong isoscalar spin-aligned pairing interaction are almost identical. We obtain a similar result: By incorporating the isoscalar spin-aligned pairing interaction in the Hamiltonian, $H'_{\rm P+Q}+V'_{P\rm max}$ predicts prominently stronger quadrupole collectivity in ^{44}Ti, especially for higher-spin states (see in Fig. 2). The isoscalar spin-aligned pairing interaction is not important.

3.2 The binding energy

Now let us focus our attention on the binding energy. We predict the binding energy of even-even nuclei using the shell model with the P+Q interactions, $H_{\rm P+Q}$, $H'_{\rm P+Q}$, and $H'_{\rm P+Q}+V'_{P1}$. We compare the binding energy between the P+Q results and the ETBME (*i.e.*, USDB and GXPF1) results, and calculate the difference between them, namely $\Delta B=B_{\rm P+Q}-B_{\rm ETBME}$. Fig. 3 presents ΔB for even-even nuclei $^{18\text{-}24}$O, $^{20\text{-}28}$Ne, $^{24\text{-}30}$Mg, $^{28\text{-}34}$Si, $^{32\text{-}36}$S, ^{36,38}Ar, $^{42\text{-}48}$Ca, $^{44\text{-}50}$Ti, $^{48\text{-}52}$Cr, and ^{52}Fe. One sees a large discrepancy between the $H_{\rm P+Q}$ and ETBME results. We extract the monopole component, $V_T(j_1j_2)$, from the pairing interactions in $H_{\rm P+Q}$ by using Eq. (4), and find that all of them are attractive. This explains the increasing ΔB as the number of valence nucleons. The change of relative energies between the single-particle orbits caused by the monopole component is not drastic, thus it does not have a significant effect on excitation energies.

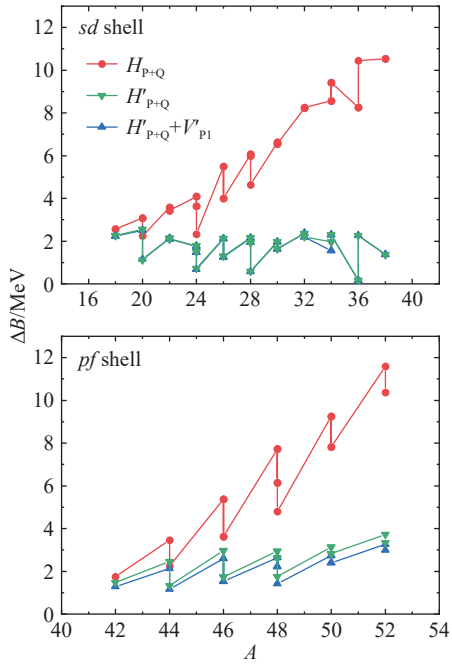

Fig. 3 (color online) The difference between the binding energy calculated by the P+Q interactions ($H_{\rm P+Q}$, $H'_{\rm P+Q}$, $H'_{\rm P+Q}+V'_{P1}$) and that by the ETBME Hamiltonian (*i.e.*, USDB and GXPF1).

The agreement between the $H'_{\rm P+Q}$ and ETBME results is much better. Yet the binding energy obtained by $H'_{\rm P+Q}$ is ~ 2 MeV larger than that by the ETBME. It is worth mentioning that the parameters of the P+Q interaction are evaluated by fitting the excitation energy data; the results can be improved if further considering the binding energy data in the fitting procedure. One might suppose that the deviation for the nuclei with $A=18$ and 42, which have 2

valence nucleons above the doubly magic cores, is attributed to single-particle energy difference between the P+Q and ETBME Hamiltonians. Indeed, in the P+Q Hamiltonian the quadrupole-quadrupole interaction contributes an additional single-particle energy term, due to the fact that the scalar product of the quadrupole operators is not a pure two-body interaction. According to out calculation, the additional single-particle energies in $H'_{\rm P+Q}$ range from -2.0 to -0.4 MeV. Considering other multipole interactions (*e.g.*, the $\sigma\tau\cdot\sigma\tau$ interaction) might compensate for the difference.

By calculating the double difference of binding energies between neighboring four nuclei, one obtains the empirical proton-neutron interaction between the last two protons and the last two neutrons in a nucleus[31–35], *i.e.*,

$$\delta V_{\rm 2p-2n}(N,Z)=\big[B(N,Z)+B(N-2,Z-2)-B(N-2,Z)-B(N,Z-2)\big]. \quad (12)$$

We calculate $\delta V_{\rm 2p-2n}$ by using the binding energies from the AME2016 data table[36] and the shell-model calculation with the P+Q and the ETBME interactions. The results are presented in Fig. 4.

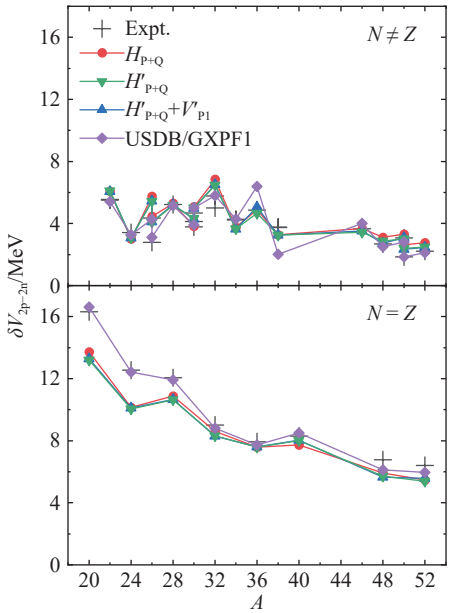

Fig. 4　(color online) The empirical proton-neutron interaction $\delta V_{\rm 2p-2n}$ calculated by using the binding energies from the AME2016 data and the shell-model calculation.

For $N\neq Z$ nuclei, $\delta V_{\rm 2p-2n}$ obtained by the P+Q interactions are in good agreement with the data or the ETBME results. In the Weizsäcker nuclear mass formula, the empirical proton-neutron interaction of $N\neq Z$ nuclei is explained by the symmetry energy[37]. In Ref. [38] the empirical proton-neutron interaction is used to constrain symmetry energy coefficients. In this work we constrain the coefficient of the I^2 volume and surface terms, $c_2^{\rm (V)}$ and $c_2^{\rm (S)}$, using the same method as in Ref. [38]. The results are presented in Table 2. We find $c_2^{\rm (V)}$ and $c_2^{\rm (S)}$ obtained by $H'_{\rm P+Q}+V'_{P1}$ are in good agreement with those constrained from experiment or the ETBME results, close to the values $c_2^{\rm (V)}=32.1$ MeV and $c_2^{\rm (S)}=58.91$ MeV suggested in Ref. [38].

Table 2　The symmetry energy and the Wigner energy coefficients extracted by using the empirical proton-neuron interaction $\delta V_{\rm 2p-2n}$ (in the unit of MeV).

Coefficient	Expt.	$H_{\rm P+Q}$	$H'_{\rm P+Q}$	$H'_{\rm P+Q}+V'_{P1}$	ETBME
$c_2^{\rm (V)}$	34.98	30.44	29.45	34.33	32.82
$c_2^{\rm (S)}$	60.51	43.30	40.36	54.13	54.50
a_W	44.45	32.52	31.21	31.18	44.01

In Fig. 4 one sees $\delta V_{\rm 2p-2n}$ for $N=Z$ nuclei is much stronger than that for their $N\neq Z$ neighbors. This significant enhancement is interpreted as a consequence of the Wigner energy[32–33, 39–40]. For even-even nuclei the Wigner energy is simply defined by

$$B_W(N,Z)=\frac{-a_W}{A}|N-Z|. \quad (13)$$

A typical value of the Wigner energy coefficient $a_W=42.7$ MeV[41]. The Wigner energy has attracted much attention in nuclear physics society. The microscopic mechanism has been studied in terms of the SU(4) spin-isospin supermultiplet theory[39–40], the seniority scheme (or the SU(2) theory)[42], the monopole and isovector pairing interactions[43–45], *etc.*

In the previous work Fu *et al.*[24] decomposed the USDB interaction into the monopole, isovector pairing, and qudrupole-quadrupole interactions, and extracted a_W for nuclei in the *sd* shell by the local mass relation, in which the binding energies were calculated using the shell model. It turned out that the value of a_W obtained with those interactions are smaller than that extracted from the experimental binding energy data. Similarly, in this work we extract a_W by using binding energies obtained with our P+Q interactions. In Fig. 4 and Table 2 one sees that $H_{\rm P+Q}$, $H'_{\rm P+Q}$, and $H'_{\rm P+Q}+V'_{P1}$ predict smaller $\delta V_{\rm 2p-2n}$ and a_W than the experimental data and the ETBME results. This indicates that residual two-body interactions beyond the P+Q interaction are indispensable to the interpretation of the Wigner energy (*e.g.*, the $\sigma\tau\cdot\sigma\tau$ interaction might be important in reproducing the isospin dependence of the binding energy[22]).

4 Summary

In this paper we study yrast states of even-even nuclei in the *sd* shell and the *pf* shell, using the shell model with the phenomenological P+Q interaction, in which the single-particle energy and the monopole interaction are taken from those in the USDB or GXPF1 interaction, and the parameters of the pairing interactions and the quadrupole-quadrupole interaction (namely, G_J and κ) are optimized by fitting excitation energy data. We find that the excitation energies of the spherical nuclei and the deformed nuclei in the *sd* (or *pf*) shell are all well reproduced by using the original P+Q interaction, $H_{\rm P+Q}$, with a unified set of parameters. However, for binding energies we see increasing discrepancy as the number of valence nucleons increases. By removing the monopole component from the pairing interactions, the prediction of binding energies is much improved. We have also shown that the isoscalar $J=1$ pairing interaction and the isoscalar spin-aligned pairing interaction are not important in our calculation.

We extract the empirical proton-neutron interaction, $\delta V_{\rm 2p-2n}$, by using the calculated binding energies, and then constrain the symmetry energy coefficients, $c_2^{(\rm V)}$ and $c_2^{(\rm S)}$, and the Wigner energy coefficient, a_W. The $\delta V_{\rm 2p-2n}$ of $N\neq Z$ nuclei and the symmetry energy coefficients obtained by the P+Q interaction agree well with those obtained from experiment, while the $\delta V_{\rm 2p-2n}$ of $N=Z$ nuclei and the Wigner energy coefficient are underestimated.

Considering other multipole interactions (*e.g.*, the hexadecapole-hexadecapole interaction, the $\sigma\tau\cdot\sigma\tau$ interaction)[1, 22–23] are reasonably expected to further improve the validity of the P+Q interaction.

References:

[1] CAURIER E, MART ÍNEZ-PINEDO G, NOWACKI F, et al. Rev Mod Phys, 2005, 77(2): 427.
[2] HJORTH-JENSEN M, KUO T T S, OSNES E. Phys Rep, 1995, 261(3): 125.
[3] BOGNER S K, KUO T T S, SCHWENK A. Phys Rep, 2003, 386(1): 1.
[4] BROWN B A. Prog Part Nucl Phys, 2001, 47(2): 517.
[5] BROWN B A, WILDENTHAL B H. Ann Rev Nucl Part Sci, 1988, 38: 29.
[6] BROWN B A, RICHTER W A. Phys Rev C, 2006, 74(3): 034315.
[7] HOMMA M, OTSUKA T, BROWN B A, et al. Phys Rev C, 2002, 65(6): 061301.
[8] HOMMA M, OTSUKA T, MIZUSAKI T, et al. Phys Rev C, 2009, 80(6): 064323.
[9] YUAN C, LIU Z, XU F, et al. Phys Lett B, 2016, 762: 237.
[10] ARIMA A, NOMURA M, KAWARADA H. Phys Lett, 1965, 19(5): 400.
[11] BARANGER M, KUMAR K. Nucl Phys A, 1968, 110(3): 490.
[12] BES D R, SORENSEN R A. The Pairing-Plus-Quadrupole Model[C]//BARANGER M, VOGT E. Advances in Nuclear Physics. Springer: New York, 1969, 2(3): 129.
[13] KISHIMOTO T, TAMURA T. Nucl Phys A, 1976, 270(2): 317.
[14] HARA K, IWASAKI S. Nucl Phys A, 1980, 348(3): 200.
[15] ZUKER A P. Nucl Phys A, 1994, 576(1): 65.
[16] HASEGAWA M, KANEKO K. Phys Rev C, 1999, 59(3): 1449.
[17] JIA L Y, ZHANG H, ZHAO Y M. Phys Rev C, 2007, 75(3): 034307.
[18] LUO Y, ZHANG Y, MENG X. Phys Rev C, 2009, 80(1): 014311.
[19] JIN H, SUN Y, KANEKO K, et al. Phys Rev C, 2013, 87(4): 044327.
[20] KANEKO K, MIZUSAKI T, SUN Y, et al. Phys Rev C, 2015, 92(4): 044331.
[21] WANG H-K, KANEKO K, SUN Y, et al. Phys Rev C, 2017, 95(1): 011304.
[22] PAN F, ZHOU D, YANG S Y, et al. Chin Phys C, 2019, 43(7): 074106.
[23] DUFOUR M, ZUKER A P. Phys Rev C, 1996, 54(4): 1641.
[24] FU G J, CHENG Y Y, JIANG H, et al. Phys Rev C, 2016, 94(2): 024312.
[25] RAE W D M. NuShellX Code[EB/OL].[2019-12-03]. http://www.garsington.eclipse.co.uk/.
[26] HESTENES M R, STIEFEL E. J Res Natl Inst Stan, 1952, 49: 409.
[27] FLETCHER R, REEVES C M. Comput J, 1964, 7: 149.
[28] FU G J, ZHAO Y M, ARIMA A. Phys Rev C, 2014, 90(5): 054333.
[29] HASEGAWA M, KANEKO K, TAZAKI S. Nucl Phys A, 2000, 674: 411.
[30] ZUKER A P, POVES A, NOWACKI F, et al. Phys Rev C, 2015, 92(2): 024320.
[31] BASU M K, BANERJEE D. Phys Rev C, 1971, 3(3): 992.
[32] VAN ISACKER P, WARNER D D, BRENNER D S. Phys Rev Lett, 1995, 74(23): 4607.
[33] BRENNER D S, WESSELBORG C, CASTEN R F, et al. Phys Lett B, 1990, 243(1-2): 1.
[34] FU G J, JIANG H, ZHAO Y M, et al. Phys Rev C, 2010, 82(3): 034304.
[35] FU G J, SHEN J J, ZHAO Y M, et al. Phys Rev C, 2013, 87(4): 044309.
[36] WANG M, AUDI G, KONDEV F G, et al. Chin Phys C, 2016, 41(3): 030003.
[37] FU G J, LEI Y, JIANG H, et al. Phys Rev C, 2011, 84(3): 034311.
[38] JIANG H, FU G J, ZHAO Y M, et al. Phys Rev C, 2012, 85(2): 024301.
[39] WIGNER E. Phys Rev, 1937, 51: 106.
[40] WIGNER E. Phys Rev, 1937, 51: 947.
[41] CHENG Y Y, BAO M, ZHAO Y M, et al. Phys Rev C, 2015, 91(2): 024313.

[42] TALMI I. Simple Models of Complex Nuclei[M]. Harwood: Harwood Academic, 1993.
[43] QI C. Phys Lett B, 2012, 717: 436.
[44] NEERGÅRD K. Phys Lett B, 2002, 537: 287.
[45] NEGREA D, SANDULESCU N. Phys Rev C, 2014, 90: 024322.

基于壳模型对力加四极力研究 sd 和 pf 壳偶偶原子核

贺冶秋, 傅冠健†

(同济大学物理科学与工程学院，上海 200092)

摘要: 本文在原子核壳模型框架下基于唯象相互作用 (对力加四极力) 研究 sd 壳和 pf 壳的偶偶核低激发集体态。在提取了 USDB 和 GXPF1 相互作用的单粒子能量和单极相互作用的基础上，我们用一套统一参数计算重现了球形核和形变核的低激发谱；将对相互作用中的单极成分扣除后可以得到较好的结合能计算结果。同位旋标量的对相互作用对计算结果影响不大。单极相互作用在经验质子—中子相互作用、原子核对称能和 Wigner 能中产生重要贡献。

关键词: 壳模型；对力加四极力；统一参数；单极成分

收稿日期: 2019-12-14；　**修改日期:** 2020-03-19
基金项目: 国家重点研发计划项目 (2018YFA0404403)；国家自然科学基金资助项目 (12075169, 11605122)
† **通信作者:** 傅冠健，E-mail：gjfu@tongji.edu.cn。